Marine Pollution Bulletin 175 (2022) 113362

Contents lists available at ScienceDirect

Marine Pollution Bulletin

journal homepage: www.elsevier.com/locate/marpolbul

Elevated pCO_2 changes community structure and function by affecting phytoplankton group-specific mortality

Peixuan Wang [a,b], Edward Laws [c], Yongzhi Wang [a,b], Jixin Chen [a,b], Xue Song [a], Ruiping Huang [a], Tifeng Wang [a], Xiangqi Yi [a], Jiazhen Sun [a], Xianghui Guo [a], Xin Liu [a,b,*], Kunshan Gao [a], Bangqin Huang [a,b]

[a] State Key Laboratory of Marine Environmental Science, Xiamen University, Xiamen, Fujian 361102, China.
[b] Fujian Provincial Key Laboratory for Coastal Ecology and Environmental Studies, Collage of the Environment and Ecology, Xiamen University, Xiamen, Fujian 361102, China.
[c] Department of Environmental Sciences, School of the Coast & Environment, Louisiana State University, Baton Rouge, LA 70803, USA.

ARTICLE INFO

Keywords:
Elevated pCO_2
Phytoplankton community structure
Mortality
Small diatoms

ABSTRACT

The rise of atmospheric pCO_2 has created a number of problems for marine ecosystem. In this study, we initially quantified the effects of elevated pCO_2 on the group-specific mortality of phytoplankton in a natural community based on the results of mesocosm experiments. Diatoms dominated the phytoplankton community, and the concentration of chlorophyll *a* was significantly higher in the high-pCO_2 treatment than the low-pCO_2 treatment. Phytoplankton mortality (percentage of dead cells) decreased during the exponential growth phase. Although the mortality of dinoflagellates did not differ significantly between the two pCO_2 treatments, that of diatoms was lower in the high-pCO_2 treatment. Small diatoms dominated the diatom community. Although the mortality of large diatoms did not differ significantly between the two treatments, that of small diatoms was lower in the high-pCO_2 treatment. These results suggested that elevated pCO_2 might enhance dominance by small diatoms and thereby change the community structure of coastal ecosystems.

1. Introduction

Under the coupled influence of global climate change and regional human activities, the biodiversity of marine communities is gradually decreasing, and the capacity of marine ecosystem to maintain the quantity and quality of their services has declined significantly. Ocean acidification (OA) caused by anthropogenic emissions of CO_2 has had major impacts on marine ecosystems. OA has been a special concern in coastal ecosystems because of the combined stresses imposed by regional eutrophication and OA knap.

Marine phytoplankton account for virtually all primary production in the ocean and play an important role in the flow of energy and the biogeochemical cycle of carbon in marine ecosystems. It is well known that 3–6% of the energetic costs of photosynthesis can be saved by down-regulating the CO_2-concentrating mechanisms (CCMs) of diatoms as CO_2 concentrations increase (Hopkinson et al., 2011). Such down-regulation has been shown to enhance the growth of the dominant coastal phytoplankton groups (diatoms and dinoflagellates) (Dutkiewicz et al., 2015), and it is generally considered to be the main factor that would cause phytoplankton growth rates, photosynthetic rates, and biomass to increase under OA conditions (Gao and Campbell, 2014). However, this enhancement of photosynthesis is expected to be small because the main source of inorganic carbon for marine phytoplankton is bicarbonate, not CO_2 (Cassar et al., 2004; Tortell et al., 2008). In addition to the positive effects associated with increased CO_2 concentrations, OA also has a negative effect associated with the decrease of pH. A reduction of pH can lead to a wide range of effects, including increased availability of metals and possibly increased metal toxicity (Shi et al., 2009). Furthermore, the decline of external pH requires increased proton pumping across the thylakoid membrane, and iron-limited conditions in the field would greatly amplify the negative effect of acidification. (Hong et al., 2017; Pörtner and Farrell, 2008). The consequence of OA is therefore the net result of both positive and negative effects. For *Trichodesmium*, a genus of cyanobacteria found in oligotrophic oceanic regions, the combined

* Corresponding author at: Fujian Provincial Key Laboratory of Coastal Ecology and Environmental Studies, Collage of the Environment and Ecology, Xiamen University, 361005, China.
E-mail address: liuxin1983@xmu.edu.cn (X. Liu).

https://doi.org/10.1016/j.marpolbul.2022.113362
Received 9 December 2021; Received in revised form 15 January 2022; Accepted 16 January 2022

effect of increasing the pCO_2 and reducing the pH is almost as bad as just reducing the pH (Hong et al., 2017). Nevertheless, it is generally believed that in eutrophic environments the positive effect associated with reducing the energetic costs of carbon fixation is greater in magnitude than the negative effect associated with reducing the pH, and the net result of elevating the pCO_2 is therefore positive (Hopkinson et al., 2011).

The strategies by which phytoplankton exploit nutrients and CO_2 differ between species (Gao and Campbell, 2014). They depend on, for example, the size, metabolic activity, and growth rates of the organisms. Because the respiration rates of dinoflagellates are higher than those of diatoms (Geider and Osborne, 1989), diatoms are more resilient to the negative impacts of reduced pH than dinoflagellates. The size of phytoplankton cells is also considered to be an important determinant of the responses of different phytoplankton to OA,whether comparisions are made between different functional groups or similar species (Gao and Campbell, 2014; Gao et al., 2012; Wu et al., 2014). Small cells tend to have larger surface/volume ratios, higher nutrient uptake rates, and higher growth rates than large cells (Edwards et al., 2012). These differences may make small cells more resilient to the stress associated with reduced pH, but they may also mean less down-regulation of CCMs (Gao and Campbell, 2014; Wu et al., 2014) and thinner boundary layers (Flynn et al., 2012). The net result of OA for small cells may therefore be negative. These net result of these inter-species differences leads to species-specific responses to OA.

Phytoplankton mortality (percentage of dead cells, %DC) is an important determinant of the dynamics of algal blooms and regulator of phytoplankton community structure (Vardi et al., 2007; Vardi et al., 2002). The causes of phytoplankton mortality fall into two categories. One category includes endogenous mechanisms such as senescent cell death and programmed cell death; the other category includes exogenous mechanisms such as grazing by herbivores, environmental stresses, viral infections, and allelopathy. Agustí and Sánchez (2002) have optimized the cell digestion assay (Darzynkiewicz et al., 1994) and have applied it to determine the percentage of living cells and dead cells in natural populations of phytoplankton. Applications of this method have revealed the response of phytoplankton mortality to environmental factors such as pH, solar radiation (Agustí, 2004; Llabrés and Agustí, 2006), and nutrient stress (Lasternas et al., 2010). Phytoplankton mortality is, not surprisingly, a function of environmental conditions (*e.g.*, pH, nutrient concentrations, and viral infection) and is a key determinant of the demise of algal blooms.

In this study, we hypothesized (1) that elevated pCO_2 could reduce mortality and increase phytoplankton biomass under eutrophic conditions and (2) that group-specific responses would lead to changes in community structure. A natural plankton community from a eutrophic bay was introduced into pre-filtered seawater to induce an algal bloom in enclosed mesocosms. During the algal bloom, phytoplankton mortality was evaluated by the cell digestion assay combined with flow cytometry (Agustí and Sánchez, 2002). We concurrently monitored environmental conditions such as pH, concentrations of nutrients and phytoplankton chlorophyll *a* (Chl-*a*), and community structure. The results demonstrated for the first time how elevated pCO_2 could affect phytoplankton community structure by differentially changing group-specific mortalities during a phytoplankton bloom.

2. Materials and methods

2.1. Experimental setup

The mesocosm experiment was conducted in the Facility for the Study of Ocean Acidification Impacts of Xiamen University (FOANIC-XMU), which is located in Wuyuan Bay (24°31′48″ N, 118°10′47″ E) in Xiamen, China. The experiment lasted from 14 April 2018 (day 0 with respect to algal inoculation) to 15 May 2018. During this period, that salinity and photoperiod were constant, the temperature increased gradually from 21.9 ± 0.1 to 26.1 ± 0.1 °C, and the daily mean photosynthetically active radiation was 690– 1075 mmol photons m^{-2} s^{-1} (Huang et al., 2021). The floating platform included 9 mesocosm enclosures. About 3000 L of prefiltered *in situ* seawater was introduced into each enclosure. A low-pCO_2 treatment (LC, 400 ppmv, bag 2, 4, 6, and 8) and high-pCO_2 treatment (HC, 1000 ppmv, bag 1, 3, 5, 7, and 9) were set up to simulate the current atmospheric pCO_2 and atmospheric pCO_2 at the end of this century respectively. To maintain the difference in the pCO_2 between the LC treatments (400 ppmv) and the HC treatments (1000 ppmv) throughout the experiment, three gas stones connected to a CO_2-enriching device (CE-100, Wuhan Ruihua Instrument & Equipment, China) were placed at the bottom of each bag. The HC treatments were continuously bubbled with an air/CO_2 mixture (1000 ppmv), whereas the LC treatments were bubbled with unenriched air (ambient pCO_2, ~400 ppmv). After the pH had stabilized, 80 L of 180-μm prefiltered *in situ* seawater were injected into each mesocosm enclosure to provide an inoculum of *in situ* communities containing viruses, bacteria, phytoplankton, and micro-zooplankton.

2.2. Environmental parameters

The pH values were determined with a spectrophotometer (Agilent 8453) and the pH indicator meta-cresol purple. The pH values were all measured on the total scale at *in situ* temperatures with measurement precision of ±0.0005 (Zhang and Byrne, 1996). The total alkalinity (TA) was calculated by the CO2SYS program from dissolved inorganic carbon (DIC) and pH (Pierrot et al., 2006) based on temperature, salinity, and measured concentrations of nutrients.

The nutrients whose concentrations we monitored included dissolved inorganic nitrogen [DIN = nitrate (NO_3^-) + nitrite (NO_2^-) + ammonium (NH_4^+)], soluble reactive phosphate (SRP), and silicate (SiO_3^{2-}). Concentrations of NO_3^-, NO_2^-, SRP, and SiO_3^{2-} were determined with a nutrient autoanalyzer (Bran+Luebbe Auto Analyzer 3, Germany) in accord with spectrophotometric protocols (Jones et al., 2005). Concentrations of NH_4^+ were measured by taking advantage of the fact that ammonia reacts with phenol in a hypochlorous acid medium to form an indophenol compound. The reaction is catalyzed by sodium nitroprusside (Pai et al., 2001). The sample was passed through a 10-mm flow cell, and the absorbance was measured at 640 nm. We reported concentrations below the detection limit as 1/2 the detection limit.

Concentrations of Chl-*a* were determined with a high-performance liquid chromatograph (HPLC)(Furuyaa et al., 2003). Before measurement, 100–200 mL of seawater were filtered through a 25-mm GF/F membrane filter (Whatman, America). The filters were stored in a freezer at −80 °C until analysis. Each filter was freeze-dried and extracted with 1 mL of *N*, *N*-dimethylformamide at −20 °C. The extract was then mixed with ammonium acetate in equal proportions. The mixed samples were assayed as soon as possible to avoid degradation of photosynthetic pigments. The total Chl-*a* concentration was equated to the sum of the concentrations of Chl-*a* and dinivyl Chl-*a*.

2.3. Phytoplankton community structure

We characterized the temporal variations of phytoplankton community structure by two methods: HPLC-CHEMTAX and Cytosub (George et al., 1989). Photosynthetic pigment concentrations were measured by high-performance liquid chromatography (HPLC) (Furuyaa et al., 2003). The relative contributions of taxa to the Chl-*a* were calculated using the CHEMTAX program (Mackey et al., 1996). Twelve diagnostic pigments were used to associate fractions of the Chl-*a* pool with eight phytoplankton groups: dinoflagellates (Dino), diatoms (Diat), haptophytes (Type 8) (Hapt_8), haptophytes (Type 6)(Hapt_6), chlorophytes (Chlo), cryptophytes (Cryp), Synechococcus (Syne), and prasinophytes (Pras)(Xiao et al., 2018). The initial input ratios of the diagnostic pigments to Chl-*a* were the same as the ratios used in previous

studies in Xiamen Bay (Liu et al., 2017). Samples were grouped based on bags. Successive runs were done to gain convergence between input and output ratios according to the CHEMTAX protocols described by Latasa (2007).

Phytoplankton were assigned to groups based on flow cytometric analysis (Cytosub, Cytobuoy b.v., Netherlands). Cytoclus software (Cytosub, Cytobuoy b.v., Netherlands) was used to cluster cells with similar optical characteristics into groups (Huang et al., 2016). The cluster analysis used basic parameters such as forward light scatter, side scatter, red fluorescence, orange fluorescence, and yellow fluorescence as well as some simple mathematical metrics of spectral signals such as inertia, asymmetry, and fill factor (Thyssen et al., 2008).

Based on CytoSub, phytoplankton cells were divided into two groups: G1 and G2. The characteristics of the G1 group were small particle size and low red fluorescence, which were considered to be diagnostic for dinoflagellates; the characteristics of the G2 group included large particle size, high red fluorescence, and a chain-like structure, which were considered to be diagnostic for chain-forming diatoms. The G2 group could be divided into large diatoms and small diatoms according to cell size (Fig. 1).

2.4. Group-specific phytoplankton mortality analysis

In situ seawater samples (15 mL) without any treatment were directly counted for total cell abundances. Viable cell abundances were determined by a cell digestion assay as modified for phytoplankton cells (Agustí and Sánchez, 2002). First, 1.5 mL of DNAse I (800 μg/mL, Sigma-Aldrich) was added to 15 mL of an *in situ* water sample and incubated at 37 °C for 15 min. Then, 1.5 mL of Trypsin (2%, Sigma-Aldrich) was added, and the sample was incubated at 37 °C for 30 min. The samples were then transferred to an ice bath for 5 min to stop enzymatic reactions, and group-specific cell abundances were quantified by Cytosub. The dead cell abundance was equated to the total cell abundance minus the viable cell abundance. Based on the Cytoclus classification results, we obtained the mortality of dinoflagellates (G1), diatoms (G2), small diatoms, and large diatoms.

2.5. Statistical analysis

Initially, outliers were identified if their modified *Z*-Score exceeded four, and then the %DC data were normalized using the Min-max normalization.

Differences between the two treatments were tested for significance with a Student's *t*-test at each point in time. For the total difference in removal, temporal effects were tested for significance by nested ANOVA, with day as a group factor and treatment as the subgroup factor. In all cases, a type I error rate (p) less than 0.05 was judged to be evidence of a significant difference.

3. Results

3.1. Environmental parameters

Throughout the experiment, the pH was significantly lower in the HC treatment than in the LC treatment (*t*-test, n = 3, $p < 0.05$, Fig. 2a). During days 8–16, the Chl-*a* concentration was significantly higher in the HC treatment than in the LC treatment (*t*-test, n = 3, $p < 0.05$), and the increase of pH was greater in the HC treatment as well. The temporal variations of the Chl-*a* concentrations showed that algal blooms occurred in each mesocosm enclosure (Fig. 2c). The different phases of the algal bloom could be identified based on the net growth rate.

(1) Days 0–6 corresponded to the initial phase of exponential growth; the Chl-*a* concentration was low (0.79–2.35 μg L^{-1}, Fig. 2c), and the pH and TA dropped by 0.17 ± 0.14 and 22.94 ± 9.81 μmol kg^{-1}, respectively, between days 0–4 (Fig. 2a, b) as a result of the decomposition of dissolved organic matter. (2) Days 6–12 corresponded to the stationary phase (Fig. 2c), during which the increase and subsequent decrease of the pH and TA indicated the cessation of positive net community production. (3) Days 12–31 corresponded to a decline phase. After the Chl-*a* concentration peaked, it abruptly dropped to 1.21 ± 0.52 μg L^{-1} on day 16. After that time, it remained stable until the end of the experiment (day 31, Fig. 2c).

The water was at first moderately eutrophic, with an ambient phosphate concentration of 0.35 ± 0.06 μmol L^{-1} (Fig. 3a). The molar nitrogen:phosphorus ratios of 52 ± 6 suggested potential phosphate limitation of phytoplankton growth (Fig. 3c). The growth of phytoplankton led to a depletion of nutrients; the phosphate and ammonium concentrations were the first to fall below the detection limits (SRP <0.08 μmol L^{-1}, NH_4^+ < 0.25 μmol L^{-1}, Fig. 3a, e) on day 2, and then the dissolved inorganic nitrogen and silicate were exhausted on day 8

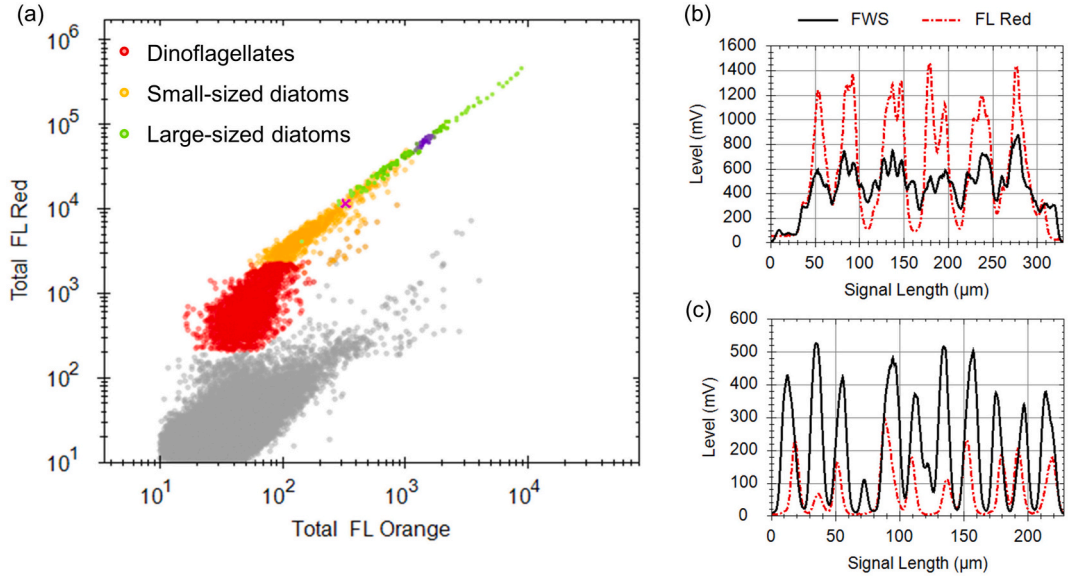

Fig. 1. Cytogram of samples (a) and the pulse shape of small-sized diatoms (b) and large-sized diatoms (c) analyzed with the CytoSub. Cytogram was obtained with a red fluorescence trigger of 30 mV. Colors in the pulse shape refer to the following signals: Forward light scatter (FWS, black) and Red Fluorescence (FL Red, red). (For interpretation of the references to colour in this figure legend, the reader is referred to the web version of this article.)

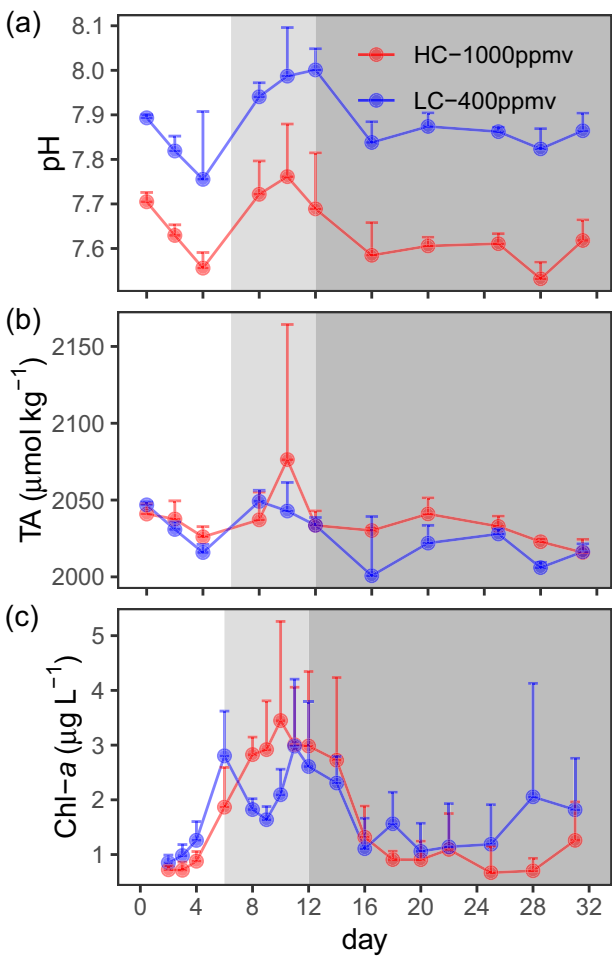

Fig. 2. Temporal variations of pH (a), total alkalinity (b) and Chl-*a* (c) concentrations in the high pCO_2 level (HC, 1000 ppmv) and low pCO_2 level (LC, 400 ppmv) treatments. The signs are the means, and the error bars are the standard error of three parallel samples.

(DIN <0.6 0 µmol L^{-1}, SiO_3^{2-} < 0.16 µmol L^{-1}, Fig. 3b, d). The nutrient stoichiometry of the whole system was strongly affected by phosphorus deficiency.

3.2. Phytoplankton community structure

Diatoms dominated the phytoplankton community structure (mean 90 ± 7% of total Chl-*a*) in the exponential and stationary phases. Dinoflagellates, which were much less abundant than diatoms, decreased from 4 ± 3% to 2 ± 1% of Chl-*a* during the exponential phase. Although there was no significant difference in the relative abundance of diatoms in the HC and LC treatments (*t*-test, n = 3, $p = 0.11$), the mean relative abundance of diatoms was higher in the HC treatment (84 ± 15%) than in the LC treatment (80 ± 17%, Fig. 4).

The total abundances detected by Cytosub revealed a progression of the algal bloom that was consistent with the Chl-*a* results ($p < 0.0001$, Fig. 5). The concentrations of the pigment characteristic of diatoms (fucoxanthin, Fuco) determined by HPLC-CHEMTAX and the abundances determined by Cytosub were consistent with each other ($p <$ 0.0001, Fig. 5). The cell sizes were significantly larger for diatoms than for dinoflagellates (Fig. 6a).

3.3. Percentages of dead cells in specific groups of phytoplankton

During the first exponential phase, the percentages of dead cells (% DC) among all phytoplankton remained low and even decreased slightly (absolute value dropped from 21 ± 0% on day 0 to 5 ± 9% on day 6; the normalized value dropped from 0.81 ± 0.04 on day 0 to 0.70 ± 0.05 on day 6). This low %DC was consistent with the increase in phytoplankton abundance and suggested that the survival of phytoplankton was good during the exponential phase (Fig. 6b). The %DC of the dinoflagellates and small diatoms exhibited a significant downward trend with time, and the %DC of large diatoms decreased from day0 to day3 (from 0.90 ± 0.00 to 0.79 ± 0.07) and then increased to 0.98 ± 0.01 at the end of the exponential phase (Fig. 6b).

The %DC values of all the phytoplankton and diatoms were significantly lower in the HC treatment than in the LC treatment (nested ANOVA, n = 60, $p < 0.05$, Fig. 6a). However, within the diatoms, only small diatoms showed a significant difference (nested ANOVA, n = 60, $p < 0.05$, Fig. 6a). The indication was that the %DC of the small diatoms largely determined the effect of elevated pCO_2 on the %DC of the diatoms *in toto*.

4. Discussion

4.1. Setup of mesocosms

There is clearly a need to bridge the gap between results from field observations and laboratory OA research (Riebesell and Tortell, 2011). Although laboratory monoculture experiments have addressed many of the mechanistic effects at the level of single cells and monospecific populations, it is difficult to extrapolate from such experiments to the level of natural communities. Mesocosms experiments have helped to fill in this gap and have shown how phytoplankton can be affected by OA at the community and even ecosystem levels (Engel et al., 2008) because they simulate the physicochemical environment of natural systems and enlarge the scale of laboratory culture studies (Riebesell et al., 2013). Many mesocosm experiments have been used to provide a link between laboratory experiments and results from field studies, especially at high latitudes (Riebesell et al., 2013; Schulz et al., 2007).

This mesocosm CO_2 perturbation experiment was carried out with water from the same eutrophic coastal bay that has been used in several previous studies (Huang et al., 2018; Lin et al., 2017; Liu et al., 2017). In this study, unlike the artificial biological communities used in the previous experiments, no extra nutrients were added, and the *in situ* biological community was used for the inoculum. The fact that organisms in the mesocosm included viruses, bacteria, phytoplankton, and zooplankton made it possible to study the response of a natural phytoplankton community to OA more realistically than would have been possible in laboratory studies. However, there are generally two problems with the use of *in situ* communities. The first problem is that the comparisons of results between treatments and controls could not be made in the way that would be possible with laboratory algal cultures. The much larger scale of mesocosms and the use of natural communities and environmental conditions add within-treatment noise that confounds comparisons between treatments and controls. Our results therefore reflect synecological rather than autecological effects. The second problem is that the duration of *in situ* observations is generally insufficient to document effects associated with genetic adaptation and evolution (Dutkiewicz et al., 2015; Lohbeck et al., 2012; Schaum et al., 2012). However, long-term exposure to the conditions of interest and high levels of replication are required if treatment effects are to be evaluated in the context of adaptation, and such studies are therefore usually performed with isolates in laboratory culture experiments. Such experimental methods are difficult to implement with communities of organisms in natural environment within which there are many complex interactions. Our experiments therefore did not account for the long-term effects of competition and the interactive effects of different limiting factors. In such cases, it is difficult to assess the trade-offs associated with the observed responses (Riebesell and Gattuso, 2014). The objective of this study was therefore to observe short-term responses to elevated pCO_2 at the community level and effects on phytoplankton

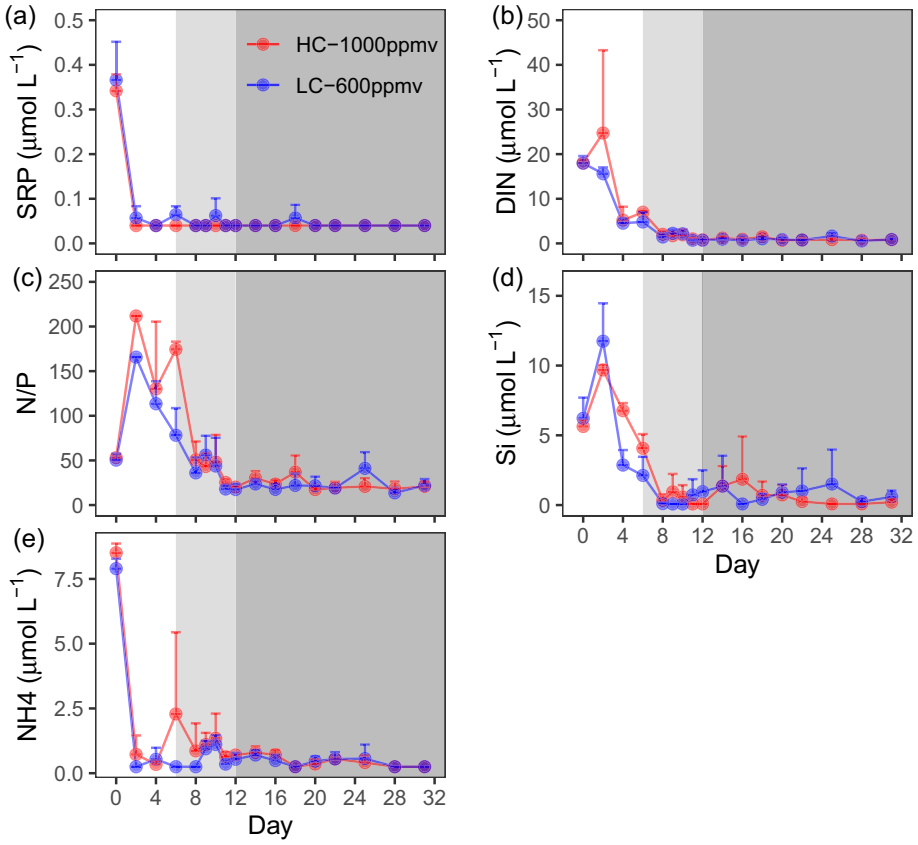

Fig. 3. Temporal variations of soluble reactive phosphate (SRP, a), dissolved inorganic nitrogen (DIN, b), N to P ratio (N/P, c), dissolved silicate (SiO_3^{2-}, d) and ammonium (NH_4^+, e) concentrations in the high pCO_2 level (HC, 1000 ppmv) and low pCO_2 level (LC, 400 ppmv) treatments. The signs are the means, and the error bars are the standard error of three parallel samples.

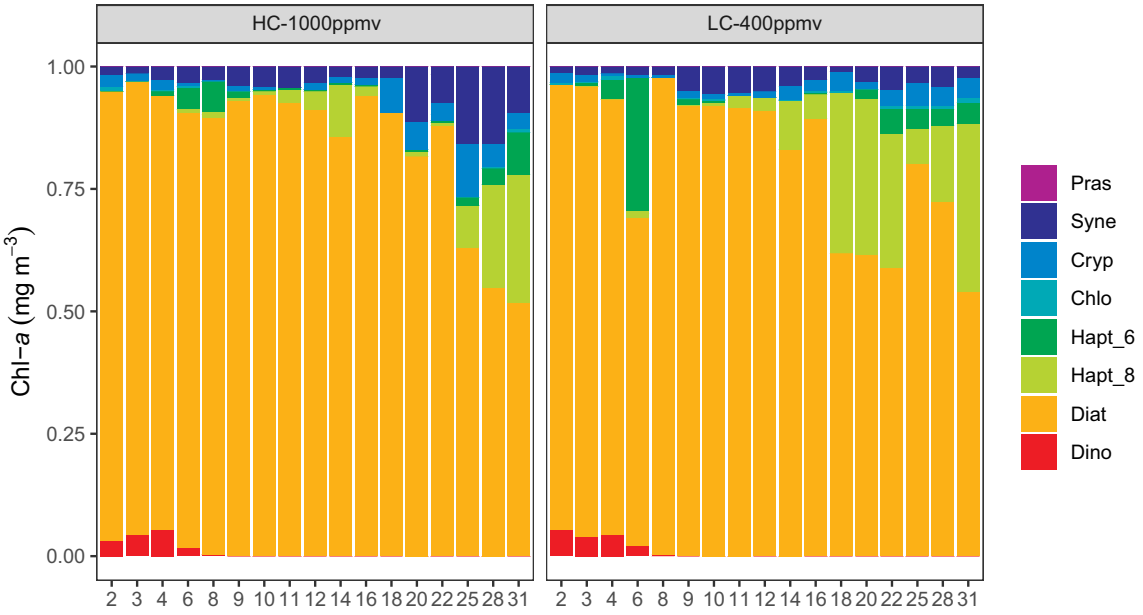

Fig. 4. Temporal variations of phytoplankton community composition in the high pCO_2 level (HC, 1000 ppmv) and low pCO_2 level (LC, 400 ppmv) treatments determined by HPLC-CHEMTAX. The Chl-*a* was contributed by eight groups: dinoflagellates (Dino), diatoms (Diat), haptophytes (Type 8)(Hapt_8), haptophytes (Type 6)(Hapt_6), chlorophytes (Chlo), cryptophytes (Cryp), Synechococcus (Syne), and prasinophytes (Pras).

mortality while maintaining natural communities (different communities of phytoplankton, bacteria, and zooplankton) and *in situ* environmental conditions (natural light and temperature changes, natural culture medium) that were as realistic as possible.

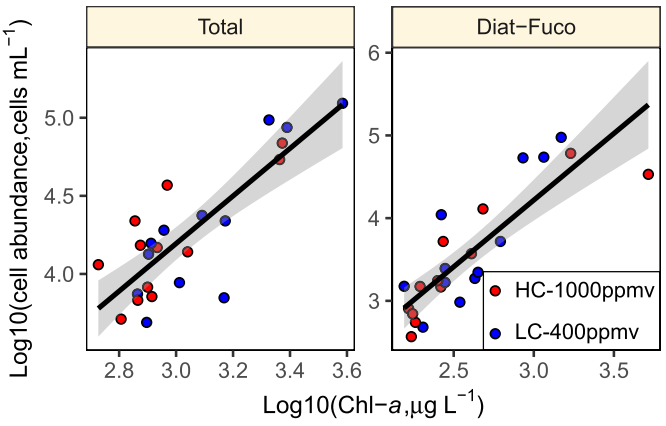

Fig. 5. Comparison of the results between Chl-*a* and total phyroplankton and diatoms abundances determined by HPLC-CHEMTAX and Cytosub in the high pCO_2 level (HC, 1000 ppmv) and low pCO_2 level (LC, 400 ppmv) treatments.

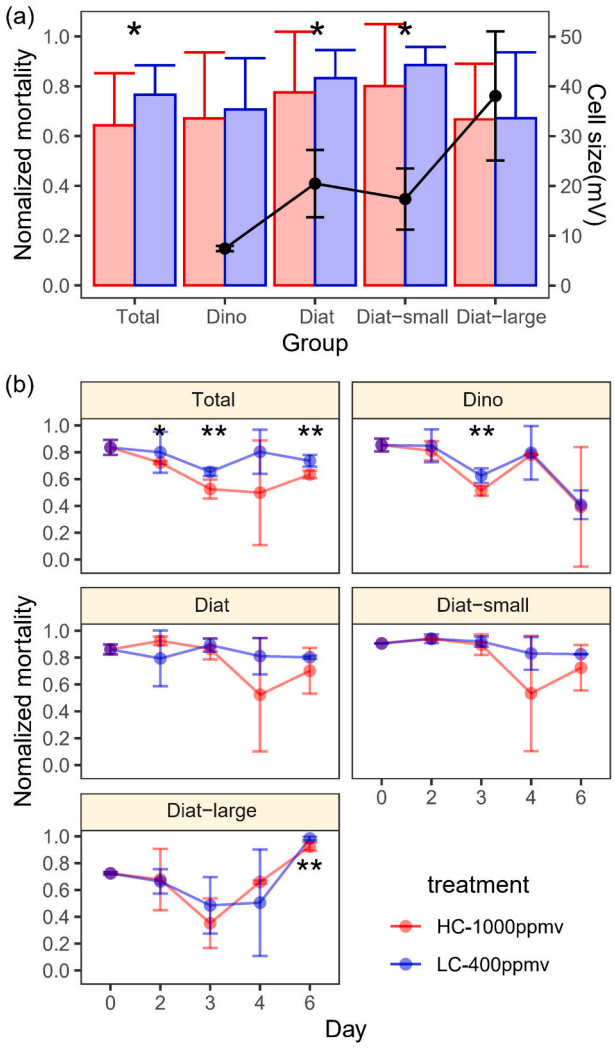

Fig. 6. The normalized mortality of total difference (a) and temporal variations (b) in total, dinoflagellates, small-sized diatoms and large-sized diatoms during the first 6 days in the high pCO_2 level (HC, 1000 ppmv) and low pCO_2 level (LC, 400 ppmv) treatmentsbased on CytoSub. The black dot represents the cell size determined by Cytosub and the asterisk represents the significant difference.

4.2. Algal bloom development

The occurrence of algal blooms was accompanied by temporal variations of pH, TA, nutrient concentrations, phytoplankton biomass, and mortality (Figs. 2, 3 and 6) under conditions of constant salinity and a cycle of photoperiodicity (Huang et al., 2021). At the beginning of the algal blooms, bacterial catabolism of large amounts of dissolved organic matter derived from terrestrial runoff released CO_2, which led to the high initial pCO_2 (~600 ppmv) in the low-pCO_2 treatment and the continuous decrease of pH (Fig. 2a) (Cai et al., 2011; Liu et al., 2017). Subsequently, the rapid growth of algae resulted in the assimilation of a large amount of dissolved inorganic carbon that changed the characteristics of the dissolved inorganic carbon system, increased the pH (Fig. 2), and rapidly consumed most of the inorganic nutrients in the water.

The ratios of the initial nutrient concentrations and order of nutrient depletion indicated that phytoplankton growth was limited by phosphate (Fig. 3a, c). This conclusion was consistent with our pervious results (Liu et al., 2017) and was also consistent with the phosphate-limitated characteristics of coastal waters due to the characteristics of terrigenous inputs (Harrison et al., 2008). The results of this experiment were therefore representative of the response of phytoplankton to elevated pCO_2 in nearshore phosphate-limited waters. The focus of this study was on the nature of that response.

There is a close connection between mortality and growth rate. Accumulating evidence (Caperon, 1969; Goldman, 1977) has shown that even in carefully controlled chemostat environments, algal populations are quite unstable at low growth rates. This instability makes it difficult to maintain steady states at low growth rates, whereas populations at higher growth rates are relatively stable. The instability may be due to increased cell mortality at low growth rates (Goldman, 1977). In our experiment, mortality was minimal (Fig. 6b) during the exponential growth period when algal reproduction was rapid (Fig. 2).

At the start of the experiment (day 0), phytoplankton had the highest %DC. The dinoflagellate %DC was only 20%, but the diatom %DC was as high as 60% (Fig. 6b). These percentages may be an accurate indication of the relative death rates of diatoms and dinoflagellates in natural waters, or they may reflect a tendency of dead diatom cells to decompose more slowly in natural waters than dead dinoflagellate cells. Alternatively, they may reflect differences between groups in sensitivity to hydrolase. However, the fact that the %DC of both diatoms and dinoflagellates declined with time (Fig. 6b) suggested that any error caused by the prior accumulation of dead diatom cells was low. However, because we could not rule out the possibility that there were differences in hydrolase sensitivity between groups, we normalized the raw %DC data to focus only on temporal variations of mortality and not on comparisons between groups.

4.3. Response of phytoplankton mortality to elevated pCO_2

The difference of mortality between the two treatment was the result of offsetting the positive and negative effects of CO_2 enrichment (Fig. 7). The positive effects of elevated pCO_2 may lower mortality, while the negative effects of reduced pH may increase mortality.

Respiration rates are relatively high for dinoflagellates *versus* diatoms (Geider and Osborne, 1989). The ratio of respiration to photosynthesis of diatoms can reach 19% during exponential growth (López-Sandoval et al., 2014). The relatively high respiration rate of dinoflagellates may be related to the energetic costs of motility and their cellular composition. The large amounts of genetic material in dinoflagellates *versus* other algae may lead to higher energetic costs associated with DNA and RNA turnover (Rizzo, 2003). The higher growth rates of diatoms *versus* dinoflagellates may therefore reflect in part the lower respiratory losses of the former (Chan, 1980; López-Sandoval et al., 2014). A decrease of extracellular pH can lead to an increase of mitochondrial respiration by affecting the redox status and

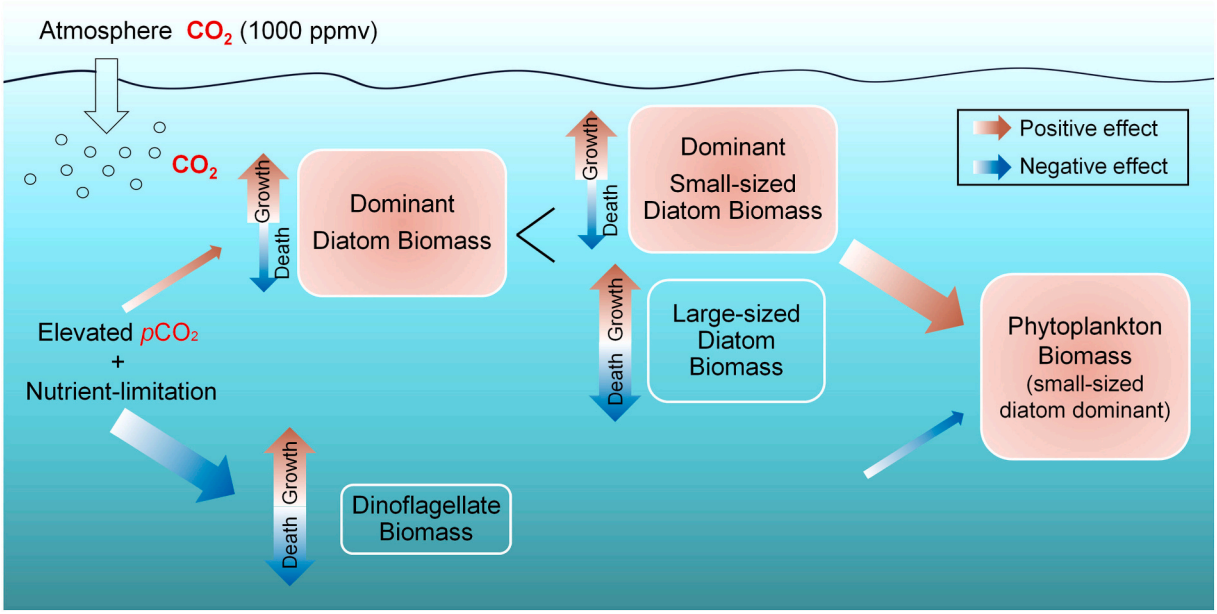

Fig. 7. Conceptual diagram illustrating the phytoplankton community response to the elevated pCO_2 in coastal water. The red arrows indicate positive (or enhance) effect, the blue arrows indicate negative (or reduce) effect. The thicker the arrow, the greater the impact. (For interpretation of the references to colour in this figure legend, the reader is referred to the web version of this article.)

ion permeability of cell membranes (Jin et al., 2015) and thereby stress phytoplankton by increasing the metabolic cost of maintaining their intracelular pH (Pörtner and Farrell, 2008). Lower pH may also reduce the ability of some species to tolerate strong ultraviolet light stress and thereby cause increased carbon losses to respiration (Gao et al., 2019; Gao et al., 2012; Laws et al., 2020). Because the respiratory losses of dinoflagellates are high even in the absence of environmental stresses, increased respiration associated with a reduction of pH may have a greater adverse effect on dinoflagellates than diatoms. An additional reason that dinoflagellates may suffer more adverse effects is that the flagellar membrane in these organisms is not covered by the cell wall. The fact that dinoflagellates must therefore constantly expend energy for regulation of volume and osmotic pressure may contribute to their higher respiration rates (López-Sandoval et al., 2014). An inability to maintain homeostasis while being stressed by reduced pH might be the main cause of dinoflagellate death in the high-pCO_2 treatment. The energy saved in acquiring CO_2 would be preferentially used to maintain intracellular homeostasis, and the mutual cancellation of the two effects could explain the fact that OA had no significant effect on the mortality of the dinoflagellates. The fact that the reduction of pH had a smaller adverse effect on the diatoms than the dinoflagellates (Fig. 6a) can probably be attributed to the high ratios of respiratoration to photosynthesis that characterize dinoflagellates.

The time series of mortality and growth rates during exponential growth (Fig. 6) allow consideration of mortality as a function of relative growth rate, *i.e.* the absolute growth rate/the maximum possible growth rate (Goldman, 1980). The lower the relative growth rate, the higher the probability of algal cell death. Small cells generally have an advantage over large cells in nutrient competition because small cells have a higher surface-to-volume ratio nutrient uptake rate, and growth rate than large cells (Edwards et al., 2012). Under phosphate-limited conditions (Fig. 3), small diatoms tend to grow at a higher percentage of their maximum growth rate than large diatoms, *i.e.*, their relative growth rate is higher. This advantage allows them to be less sensitive to the adverse effects of reduced pH than large cells. The result is a lower probability of their dying.

The positive effects of elevated pCO_2 are greater for large diatoms than small diatoms becuse large cells have a relatively small surface/volume ratio, a longer distance between the chloroplast and cell membrane, and hence greater difficulty in maintaining high intracellular levels of CO_2. It is consequently often the case that CCMs are down-regulated more in relatively large cells (*e.g.*, some diatoms and dinoflagellates) under high CO_2-conditions, and the benefit of high CO_2 concentrations to large phytoplankton may be especially apparent at such times (Gao and Campbell, 2014; Wu et al., 2014). However, these previous results have all been obtained with laboratory cultures under nutrient-replete conditions. Under such conditions, the relative growth rates of both the large and small diatoms are identical and equal to 1. The reason the relative growth rates of the large cells increase more in the transition from nutrient-limited to nutrient-replete conditions is that the relative growth rates of the large cells are lower than those of the small cells under nutrient-limited conditions (Goldman, 1980), thus the mortality of the large cells would be higher than those of the small cells. The results of this study reflected the differential response of the mortality of large and small diatoms in the transition from phosphate-limited growth to growth under nutrient-replete conditions. The relative growth rates of the large diatoms were lower under nutrient-limited conditions, and thus they were less tolerant than the small diatoms under phosphate-limited conditions to the adverse effects of reduced pH.

4.4. *Response of Chl-a and phytoplankton community to elevated pCO_2*

The consistent differences of pH and carbonate system characteristics (Huang et al., 2021) between the HC and LC treatments meant that phytoplankton in the HC treatment were affected by elevated pCO_2 throughout the experiment, although the pH increased significantly as the photosynthetic rates increased (Fig. 2a). Consistent with most previous studies, the Chl-*a* concentration was higher in the HC treatments than the LC treatments (Fig. 2c). Theortically, this difference of Chl-*a* concentrations may be caused by two factors: an increase of primary production (Engel et al., 2013) and a reduction of death rates. Although a significant increase of primary production in HC treatments has been observed in previous mesocosm enclosure experiments at the same facility (Huang et al., 2018), an increase of primary production was not detected in this experiment (Huang et al., 2021). Instead, there was a reduction of mortality (Fig. 6a). The implication is that the increase of the Chl-*a* concentrations in this experiment was caused by a reduction of phytoplankton mortality rather than an increase of primary production.

This difference might have been due to the relatively nutrient-deficient conditions of this study. Downregulation of CCMs can lead to a reduction of the energetic costs of carbon acquisition by 3–6% (Hopkinson et al., 2011). That reduction might have a positive effect on phytoplankton biomass. Valenzuela et al. (2018) have concluded that under HC conditions, the energy saved during the growth of phytoplankton could enhance viability if it were used for physiological state transformations or alleviation of potential environmental stress. It could be used, for example, to up-regulate the expression of nitrite reductase (nir) (Li et al., 2017) and alkaline phosphatase (AP) (Tanaka et al., 2008) under nutrient-limited conditions. Under nutrient-limited conditions, phytoplankton may not have enough energy to increase primary production and combat the effects of a reduction of pH at the same time. A reduction of mortality may thus be the response of phytoplankton to HC conditions when growth rates are limited by nutrients.

The results of the phytoplankton community structure analyses showed that the increased Chl-*a* was contributed mainly by diatoms (Fig. 4), and diatom mortality was significantly reduced in the HC treatment (Fig. 6a). We therefore have sufficient reason to infer that when diatoms dominate a phytoplankton community in coastal water with high biomass, the increase of phytoplankton biomass is facilitated by a reduction of diatom mortality (Fig. 7). This conclusion is a very important result of this study. The results confirmed a positive effect of CO_2 enrichment on phytoplankton biomass. This effect was evidenced for the first time in the mortality of different phytoplankton species and cell sizes. If this response proves to be consistent, elevated pCO_2 may change the composition of phytoplankton communities by its differential effects on phytoplankton mortality (Fig. 7).

Our results showed that OA may not only increase the biomass of primary producers (Fig. 2b) but also lead to changes of phytoplankton community structure (Fig. 4) by altering the mortality of specific groups of phytoplankton (Fig. 6). OA may therefore affect not only the biomass but also the taxonomic composition and functionality of planktonic communities (Doney et al., 2020). Under OA conditions, most organisms contribute to only a few functional roles. The functionality of species is therefore characterized by a low level of redundancy (Doney et al., 2020). OA may therefore have a rather direct impact on the functional roles of different taxa (Teixido et al., 2018). However, studies have shown that even if the CO_2 concentration reaches 2000 μatm, it is unlikely to reduce ecological functionality if tolerant species can replace sensitive and vulnerable species (Baggini et al., 2015). The abundance of diatoms, which appear to be relatively resilient to future ocean acidification conditions, will be enhanced (Valenzuela et al., 2018). Ocean acidification may therefore cause unexpected responses at the community level.

5. Conclusions

This study reported for the first time an effect of elevated pCO_2 on the mortality and community structure of phytoplankton. We successfully conducted mesocosm enclosure experiments with two pCO_2/pH treatments in a coastal region to simulate algal bloom events under current atmospheric pCO_2 and the atmospheric pCO_2 predicted at the end of this century. The results showed that (1) CO_2 enrichment led to higher Chl-*a* concentrations; (2) the increased Chl-*a* was contributed mainly by diatoms; (3) elevated CO_2 decreased the mortality of the small diatoms. These results indicated that elevation of CO_2 may stimulate algal biomass and enhance the dominance of small diatoms by reducing their mortality in coastal ecosystems.

CRediT authorship contribution statement

Peixuan Wang: Conceptualization, Formal analysis, Writing – original draft, Methodology, Software. **Edward Laws:** Writing – review & editing, Supervision. **Yongzhi Wang:** Investigation. **Jixin Chen:** Methodology, Software. **Xue Song:** Investigation. **Ruiping Huang:** Resources. **Tifeng Wang:** Resources. **Xiangqi Yi:** Resources. **Jiazhen Sun:** Resources. **Xianghui Guo:** Data curation, Supervision. **Xin Liu:** Conceptualization, Formal analysis, Writing – review & editing. **Kunshan Gao:** Data curation, Supervision. **Bangqin Huang:** Data curation, Supervision.

Declaration of competing interest

The authors declare that they have no known competing financial interests or personal relationships that could have appeared to influence the work reported in this paper.

Acknowledgments

This work was supported by the National Natural Science Foundation of China [grant numbers 41776146, 42122044, U1805241, 41706139], the National Key Research and Development Program of China [grant number 2016YFA0601203], and the Programme of Introducing Talents of Discipline to Universities ("111" Project) [grant number BP0719030]. Project supported by Southern Marine Science and Engineering Guangdong Laboratory (Zhuhai) (No. SML2021SP308) were acknowledged. We would like to thank Heng Zhu, Xinrui Shen and Qian Qi for help with the data collection. We are also grateful to the technical supporting staff, Xiaowen Jiang, Di Zhang, He Li, Xiangqi Yi, Souchang Chen, Nanou Bao, Liming Qu, Xin Lin.

References

Agustí, S., 2004. Viability and niche segregation of *Prochlorococcus* and *Synechococcus* cells across the Central Atlantic Ocean. Aquat. Microb. Ecol. 36, 53–59.
Agustí, S., Sánchez, M.C., 2002. Cell viability in natural phytoplankton communities quantified by a membrane permeability probe. Limnol. Oceanogr. 47, 818–828.
Baggini, C., Issaris, Y., Salomidi, M., Hall-Spencer, J., 2015. Herbivore diversity improves benthic community resilience to ocean acidification. J. Exp. Mar. Biol. Ecol. 469, 98–104.
Cai, W.-J., Hu, X., Huang, W.-J., Murrell, M.C., Lehrter, J.C., Lohrenz, S.E., et al., 2011. Acidification of subsurface coastal waters enhanced by eutrophication. Nat. Geosci. 4, 766–770.
Caperon, J., 1969. Time lag in population growth response of *Isochrysis Galbana* to a variable nitrate environment. Ecology 50, 198-192.
Cassar, N., Laws, E.A., Bidigare, R.R., Popp, B.N., 2004. Bicarbonate uptake by Southern Ocean phytoplankton. Glob. Biogeochem. Cycles 18 n/a-n/a.
Chan, A.T., 1980. Comparative physiological study of marine diatoms and dinoflagellates in relation to irradiance and cell size. II. Relationship between photosynthesis, growth, and carbon/chlorophyll a ratio. J. Phycol. 16, 428–432.
Darzynkiewicz, Z., Li, X., Gong, J., 1994. Chapter 2 assays of cell viability: discrimination of cells dying by apoptosis. In: Flow Cytometry Second Edition, Part A, pp. 15–38.
Doney, S.C., Busch, D.S., Cooley, S.R., Kroeker, K.J., 2020. The impacts of ocean acidification on marine ecosystems and reliant human communities. Annu. Rev. Environ. Resour. 45, 83–112.
Dutkiewicz, S., Morris, J.J., Follows, M.J., Scott, J., Levitan, O., Dyhrman, S.T., et al., 2015. Impact of ocean acidification on the structure of future phytoplankton communities. Nat. Clim. Chang. 5, 1002–1006.
Edwards, K.F., Thomas, M.K., Klausmeier, C.A., Elena, L., 2012. Allometric scaling and taxonomic variation in nutrient utilization traits and maximum growth rate of phytoplankton. Limnol. Oceanogr. 57, 554–566.
Engel, A., Schulz, K., Riebesell, U., Bellerby, R., Delille, B., Schartau, M., 2008. Effects of CO_2 on particle size distribution and phytoplankton abundance during a mesocosm bloom experiment (PeECE II). Biogeosciences 5, 509–521.
Engel, A., Borchard, C., Piontek, J., Schulz, K., Riebesell, U., Bellerby, R., 2013. CO_2 increases ^{14}C primary production in an Arctic plankton community. Biogeosciences 10, 1291–1308.
Flynn, K.J., Blackford, J.C., Baird, M.E., Raven, J.A., Clark, D.R., Beardall, J., et al., 2012. Changes in pH at the exterior surface of plankton with ocean acidification. Nat. Clim. Chang. 2, 510–513.
Furuyaa, K., Hayashia, M., Yabushitab, Y., Ishikawa, A., 2003. Phytoplankton dynamics in the East China Sea in spring and summer as revealed by HPLC-derived pigment signatures. Deep-Sea Research II 50, 367–387.
Gao, K., Campbell, D.A., 2014. Photophysiological responses of marine diatoms to elevated CO_2 and decreased pH: a review. Funct. Plant Biol. 41, 449–459.
Gao, K., Helbling, E.W., Häder, D.P., Hutchins, D.A., 2012. Responses of marine primary producers to interactions between ocean acidification, solar radiation, and warming. Mar. Ecol. Prog. Ser. 470, 167–189.
Gao, K., Beardall, J., Häder, D.-P., Hall-Spencer, J.M., Gao, G., Hutchins, D.A., 2019. Effects of ocean acidification on marine photosynthetic organisms under the concurrent influences of warming, UV radiation, and deoxygenation. Frontiers in marineScience 6.

Geider, R.J., Osborne, B.A., 1989. Respiration and microalgal growth: a review of the quantitative relationship between dark respiration and growth. New Phytol. 112, 327–344.
George, D., Groenewegen, A.C., Willem, S., GJvd, Engh, JWM, Visser, 1989. The optical plankton analyser (O.P.A.): a flow cytometer for plankton analysis, II: specifications. Cytometry 10, 529–539.
Goldman, J.C., 1977. Steady state growth of phytoplankton in continuous culture: comparison of internal and external nutrient equations 1,2. J. Phycol. 13, 251–258.
Goldman, J.C., 1980. Primary productivity in the sea. In: Falkowski, P.G. (Ed.), Physiological Processes, Nutrient Availability, and the Concept of Relative Growth Rate in Marine Phytoplankton Ecology. Springer, Boston, MA.
Harrison, P.J., Yin, K., Lee, J.H.W., Gan, J., Liu, H., 2008. Physical–biological coupling in the Pearl River Estuary. Cont. Shelf Res. 28, 1405–1415.
Hong, H., Shen, R., Zhang, F., Wen, Z., Chang, S., Lin, W., et al., 2017. The complex effects of ocean acidification on the prominent N_2-fixing cyanobacterium Trichodesmium. Science 356, 527–531.
Hopkinson, B.M., Dupont, C.L., Allen, A.E., Morel, F.M., 2011. Efficiency of the CO_2-concentrating mechanism of diatoms. Proc. Natl. Acad. Sci. U. S. A. 108, 3830–38377.
Huang, X., Liu, X., Chen, J., Xiao, W., Cao, Z., Huang, B., 2016. Seasonal variations of group-specific phytoplankton cell death in Xiamen Bay, China. Chin. J. Oceanol. Limnol. 35, 324–335.
Huang, Y., Liu, X., Laws, E.A., Chen, B., Li, Y., Xie, Y., et al., 2018. Effects of increasing atmospheric CO_2 on the marine phytoplankton and bacterial metabolism during a bloom: a coastal mesocosm study. Sci. Total Environ. 633, 618–629.
Huang, R., Sun, J., Yang, Y., Jiang, X., Wang, Z., Song, X., et al., 2021. Elevated pCO_2 impedes succession of phytoplankton community from diatoms to dinoflagellates along with increased abundance of viruses and bacteria. Front. Mar. Sci. 8.
Jin, P., Wang, T., Liu, N., Dupont, S., Beardall, J., Boyd, P.W., et al., 2015. Ocean acidification increases the accumulation of toxic phenolic compounds across trophic levels. Nat. Commun. 6.
Jones, R.M., Bye, C.M., Dold, P.L., 2005. Nitrification parameter measurement for plant design: experience and experimental issues with new methods. Water Sci. Technol. 52, 461–468.
Lasternas, S., Agustí, S., Duarte, C.M., 2010. Phyto- and bacterioplankton abundance and viability and their relationship with phosphorus across the Mediterranean Sea. Aquat. Microb. Ecol. 60, 175–191.
Latasa, M., 2007. Improving estimations of phytoplankton class abundances using CHEMTAX. Mar. Ecol. Prog. Ser. 329, 13–21.
Laws, E.A., Mc, C.S.A., Passow, U., 2020. Interactive effects of CO_2, temperature, irradiance, and nutrient limitation on the growth and physiology of the marine diatom *Thalassiosira pseudonana* (Coscinodiscophyceae). J. Phycol. 56, 1614–1624.
Li, Y., Zhuang, S., Wu, Y., Ren, H., Chen, F., Lin, X., et al., 2017. Ocean acidification modulates expression of genes and physiological performance of a marine diatom. PLoS One 12, e0170970.
Lin, X., Huang, R., Li, Y., Wu, Y., Hutchins, D.A., Dai, M., et al., 2017. Insignificant effects of elevated CO_2 on bacterioplankton community in a eutrophic coastal mesocosm experiment. Biogeosci. Discuss. 15, 1–36.
Liu, X., Li, Y., Wu, Y., Huang, B., Dai, M., Fu, F., et al., 2017. Effects of elevated CO_2 on phytoplankton during a mesocosm experiment in the southern eutrophicated coastal water of China. Sci. Rep. 7, 6868.
Llabrés, M., Agustí, S., 2006. Picophytoplankton cell death induced by UV radiation: evidence for oceanic Atlantic communities. Limnol. Oceanogr. 51, 21–29.
Lohbeck, K.T., Riebesell, U., Reusch, T.B.H., 2012. Adaptive evolution of a key phytoplankton species to ocean acidification. Nat. Geosci. 5, 346–351.
López-Sandoval, D.C., Rodríguez-Ramos, T., Cermeño, P., Sobrino, C., Marañón, E., 2014. Photosynthesis and respiration in marine phytoplankton: relationship with cell size, taxonomic affiliation, and growth phase. J. Exp. Mar. Biol. Ecol. 457, 151–159.
Mackey, M.D., Mackey, D.J., Higgins, H.W., Wrighit, S.W., 1996. CHEMTAX- a program for estimating class abundances from chemical markers: application to HPLC measurements of phytoplankton. Mar. Ecol. Prog. Ser. 144, 265–283.
Pai, S.C., Tsau, Y.J., Yang, T., 2001. pH and buffering capacity problems involved in the determination of ammonia in saline water using the indophenol blue spectrophotometric method. Anal. Chim. Acta 434, 209–216.
Pierrot, D., Lewis, E., Wallace, R., Wallace, D., Wallace, W., Wallace, D., 2006. MS Excel Program Developed For CO_2 System Calculations. Carbon Dioxide Information Analysis Center, Oak Ridge National Laboratory, U.S. Department of Energy.
Pörtner, H.-O., Farrell, A., 2008. Physiology and climate change. Science 322, 690–692.
Riebesell, U., Gattuso, J.-P., 2014. Lessons learned from ocean acidification research. Nat. Clim. Chang. 5, 12–14.
Riebesell, U., Tortell, P.D., 2011. Effects of ocean acidification on pelagic organisms and ecosystems. In: Gattuso, J.-P., Hansson, L. (Eds.), Ocean Acidification. Oxford University Press, Oxford, pp. 99–121.
Riebesell, U., Gattuso, J.P., Thingstad, T.F., Middelburg, J.J., 2013. Preface"Arctic Ocean acidification: pelagic ecosystem and biogeochemical responses during a mesocosm study". Biogeosciences 10, 5619–5626.
Rizzo, P.J., 2003. Those amazing dinoflagellate chromosomes. Cell Res. 13, 215–217.
Schaum, E., Rost, B., Millar, A.J., Collins, S., 2012. Variation in plastic responses of a globally distributed picoplankton species to ocean acidification. Nat. Clim. Chang. 3, 298–302.
Schulz, K.G., Riebesell, U., Bellerby, R.G.J., Biswas, H., Meyerhöfer, M., Müller, M.N., et al., 2007. Build-up and decline of organic matter during PeECE III. Biogeosci. Discuss. 4, p4539.
Shi, D., Xu, Y., Morel, F.M.M., 2009. Effects of the pH/ pCO_2 control method on medium chemistry and phytoplankton growth. Biogeosciences 6, 1199–1207.
Tanaka, T., Thingstad, T.F., Løvdal, T., Grossart, H.P., Larsen, A., Allgaier, M., et al., 2008. Availability of phosphate for phytoplankton and bacteria and of glucose for bacteria at different pCO_2 levels in a mesocosm study. Biogeosciences 5, 669–678.
Teixido, N., Gambi, M.C., Parravacini, V., Kroeker, K., Micheli, F., Villeger, S., et al., 2018. Functional biodiversity loss along natural CO_2 gradients. Nat. Commun. 9, 5149.
Thyssen, M., Mathieu, D., Garcia, N., Denis, M., 2008. Short-term variation of phytoplankton assemblages in Mediterranean coastal waters recorded with an automated submerged flow cytometer. J. Plankton Res. 30, 1027–1040.
Tortell, P.D., Payne, C., Gueguen, C., Strzepek, R.F., Boyd, P.W., Rost, B., 2008. Inorganic carbon uptake by Southern Ocean phytoplankton. Limnol. Oceanogr. 53, 1266–1278.
Valenzuela, J.J., Garcia, Lopez, de Lomana, A., Lee, A., Armbrust, E.V., Orellana, M.V., Baliga, N.S., 2018. Ocean acidification conditions increase resilience of marine diatoms. Nat. Commun. 9, 2328.
Vardi, A., Schatz, D., Beeri, K., Motro, U., Sukenik, A., Levine, A., et al., 2002. Dinoflagellate-cyanobacterium communication may determine the composition of phytoplankton assemblage in a mesotrophic lake. Curr. Biol. 12, 1767–1772.
Vardi, A., Eisenstadt, D., Murik, O., Berman-Frank, I., Zohary, T., Levine, A., et al., 2007. Synchronization of cell death in a dinoflagellate population is mediated by an excreted thiol protease. Environ. Microbiol. 92, 360–369.
Wu, Y., Jeans, J., Suggett, D.J., Finkel, Z.V., Campbell, D.A., 2014. Large centric diatoms allocate more cellular nitrogen to photosynthesis to counter slower RUBISCO turnover rates. Front. Mar. Sci. 1.
Xiao, W., Wang, L., Laws, E., Xie, Y., Chen, J., Liu, X., et al., 2018. Realized niches explain spatial gradients in seasonal abundance of phytoplankton groups in the South China Sea. Prog. Oceanogr. 162, 223–239.
Zhang, H., Byrne, R., 1996. Spectrophotometric pH measurements of surface seawater at in-situ conditions: absorbance and protonation behavior of thymol blue. Mar. Chem. 52, 17–25.